BIOCHEMISTRY
including biophysical chemistry & molecular biology

Article

pubs.acs.org/biochemistry

Loop Sequence Dictates the Secondary Structure of a Human Membrane Protein Hairpin

Vincent G. Nadeau and Charles M. Deber*

Program in Molecular Structure and Function, Research Institute, Hospital for Sick Children, Toronto M5G 1X8, Ontario, Canada, and Department of Biochemistry, University of Toronto, Toronto M5S 1A8, Ontario, Canada

Supporting Information

ABSTRACT: Membrane proteins adopt two fundamental types of folds in nature: membranes in all organisms harbor α-helical bundles linked by extramembranous loops of varying length, while β-barrel structures are found in the outer membrane of Gram-negative bacteria, mitochondria, and chloroplasts. Here we report that turn-inducing loop mutations in a transmembrane hairpin induce the conversion of an α-helical hairpin to β-sheet oligomers in membrane environments. On the basis of an observation of a sequence bias toward Pro and Gly in the turns of native β-barrel membrane proteins, we characterized in sodium dodecyl sulfate (SDS) micelles and 1-palmitoyl-2-oleoyl-*sn*-glycero-3-phosphocholine (POPC) bilayers several "hairpin" constructs of cystic fibrosis transmembrane conductance regulator transmembrane segments 3 and 4 (TM3−loop−TM4; loop region being ^{215}IWELLQASA^{223}) in which Pro-Gly residues were either inserted or substituted at several positions. Remarkably, suitable positioning of the Pro-Gly doublet caused the adoption of stable β-sheet structures by several mutants in SDS micelles, as shown by circular dichroism spectroscopy, concurrent with a ladder of discrete oligomers observed via SDS−polyacrylamide gel electrophoresis. Reconstitution of wild-type (WT) TM3/4 into POPC vesicles studied by Trp fluorescence, in conjunction with positional quenchers in brominated phospholipids, indicated a transbilayer position for helical WT TM3/4, but likely a largely surface-embedded conformation for the β-sheet mutant with loop region IW*P*G*E*LLQASA. To the best of our knowledge, such a complete change in the fold with a minimal number of mutations has not been previously observed for a membrane protein. These facile α-helix to β-sheet conversions highlight the contribution of loops to membrane protein structure.

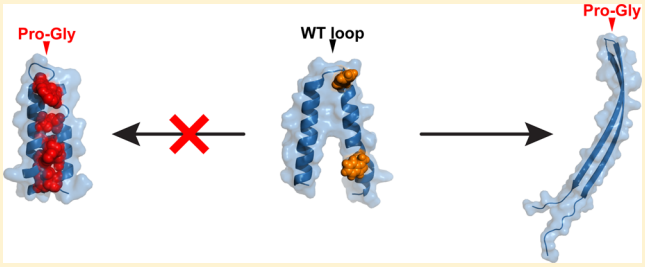

Membrane proteins adopt two types of structure in the core hydrophobic environment of lipid bilayers: α-helical segments/bundles and β-barrels. α-Helical membrane proteins are found across all kingdoms of life and in all lipid bilayers; β-barrels are exclusive to the outer membranes of Gram-negative bacteria and of endosymbiont organelles, i.e., mitochondria and chloroplasts. Structurally, each of these folds allows membrane proteins to dampen the polarity of backbone amide and carbonyl groups through H-bonding and sequester them from the acyl tails of lipids, leaving hydrophobic side chains available to interact with the surrounding environment. The sequences of β-barrels and α-helical bundles are each characterized by a series of transmembrane (TM) segments that span the bilayer as β-strands or as α-helices that are linked by loop regions that exit the hydrophobic core of the lipid bilayer, resulting in a collapsed and compact structure in the lipid bilayer.

Extensive mutagenesis of membrane-embedded segments has highlighted key sequence requirements for proper folding,[1−4] but data regarding any specific role of loop sequences in dictating the final fold of a membrane protein remain limited. Previous studies suggest that loop sequences contribute to the stability of membrane protein folds. For example, while the loops of bacteriorhodopsin do not have to be intact for this helical bundle protein to fold,[5,6] they are required for stability.[7,8] In mammalian rhodopsin, extramembranous loops must be preserved for proper folding[9] and function.[10] Thus, certain membrane proteins contain tailored loop sequences that allow them to fold to their native structure.

The demonstration of a role for loop regions in establishing native membrane protein stability implies that these extramembranous sequences may contribute to protein folding by adopting sequence-dependent conformations that impact the adjacent membrane-embedded regions. This idea is supported by the ability of peptides derived from the sequence of membrane protein loops to adopt turnlike structures[11−14] in membrane-mimetic environments. In fact, some loop peptides, for example, those from bacteriorhodopsin[14] and the hairpin of subunit c from ATP synthase,[11] form turns very similar to their structure in the full-length parent proteins. Thus, one would expect that loops with such a sequence should impact the proximity and folding of the segments they connect. This property of loop regions has been demonstrated in numerous

Received: February 13, 2013
Revised: March 13, 2013
Published: March 14, 2013

dx.doi.org/10.1021/bi400187w | *Biochemistry* 2013, 52, 2419−2426

instances in water-soluble proteins in which short turns can strongly impact the thermodynamics and kinetics of folding.[15] In addition, the formation of such turns is strongly dependent on sequence, with specific residue requirements known to promote various turn types.[16]

Here we sought to further investigate the impact of loop sequence changes on the structure of membrane proteins in an α-helical hairpin model consisting of a helix−loop−helix construct composed of transmembrane segments 3 and 4 from the human cystic fibrosis transmembrane conductance regulator (CFTR TM3/4) with a relatively short predicted extracellular loop.[17] The Pro-Gly doublet, a short sequence that strongly promotes β-turns in water-soluble proteins,[16] was introduced at various positions in the TM3/4 loop sequence, and the structural impact of this sequence alteration was evaluated by circular dichroism and fluorescence spectroscopy, polyacrylamide gel electrophoresis, and size-exclusion chromatography. We found that Pro-Gly loop mutations were capable of inducing a change in the structure of the TM3/4 membrane-spanning regions in several instances, causing a complete structural conversion from a monomeric α-helical species to a series of discrete β-sheet oligomers. Our results indicate that small changes in loop sequence have the capacity to cause structural transitions in transmembrane regions, and further support a role for loops in influencing the type and stability of membrane protein folds.

EXPERIMENTAL PROCEDURES

Residue Frequency in Short Turns of β-Barrels. A list of 48 nonredundant β-barrel structures and corresponding Protein Data Bank (PDB) files were downloaded from the PDBTM (http://pdbtm.enzim.hu/) and the RCSB Protein Data Bank (http://www.pdb.org) in February 2011. The structures were subdivided into 623 strand−loop−strand structural subunits, termed "β-hairpins". β-Hairpins were structurally aligned in SwissPDB viewer (http://spdbv.vital-it.ch) by minimizing the backbone root-mean-square deviation values of the three residues that (i) were identified by SwissPDB viewer as conforming to β-strand ϕ and ψ angles and (ii) immediately preceded or followed a nonstrand structural region where the polypeptide chain changed direction by ∼180°. The six resulting structurally aligned β-strand residues and the intervening nonstrand region were termed "anchor" and "turn" sequences, respectively. For sequence analysis, turns were divided into categories on the basis of their length [2-residue (n = 110), 3-residue (n = 161), 4-residue (n = 44), or ≥5-residue turns (n = 308)] and the frequency of occurrence of each of the 20 canonical amino acid residues at each turn position in the 2- and 3-residue categories was calculated. Statistical significance of residue distributions was evaluated in Microsoft Excel by comparing the observed counts for all residues to the counts expected if residues were randomly distributed at each turn position. Cys and Met were excluded from the analysis on the basis of their low frequency of occurrence in the database.

Expression and Purification of TM3/4 Hairpin Constructs. Mutagenesis was performed using the QuikChange site-directed mutagenesis kit (Stratagene), and proteins were expressed and purified essentially as described previously,[17] with the exceptions of expressing the protein in small-scale (250 mL) M9 minimal medium cultures and inducing expression for 18−20 h at 25 or 16 °C. TM3/4 constructs were purified from their thioredoxin tag after thrombin cleavage by reverse-phase high-performance liquid chromatography (RP-HPLC) on a C4 semipreparative or preparative column (Phenomenex). A biphasic gradient was used for complete separation of hairpins from contaminants with a first-exponential gradient step from water to acetonitrile and a second linear gradient step from acetonitrile to 2-propanol. Mass spectrometry-verified elution peaks were lyophilized before further use. The sequence of the wild-type 87-residue hairpin construct is GSGMKETAAAKFERQHMDSPDLGTDDDDCKAM^{194}GLALAHFVWIAPLQVALLMGLIWELLQASAFAGLGFLIVLALFQAGLG^{241}LECHHHHH, which embeds human CFTR residues 194−241 along with purification tags from the vector.[17]

Solubilization of TM3/4 Hairpins in Detergent Micelles and in Lipid Bilayers. Freeze-dried powders of TM3/4 constructs were initially solubilized in 1,1,1,3,3,3-hexafluoro-2-propanol (HFIP) by sonication for 10 min, after which HFIP was evaporated with N_2 gas. The HFIP-treated TM3/4 hairpins were then reconstituted in 0.3% SDS and 50 mM sodium phosphate (pH 7) and quantitated using the micro BCA assay (Thermo Fisher).

For reconstitution into lipid bilayers, 1-palmitoyl-2-oleoyl-*sn*-glycero-3-phosphocholine (POPC) lipid stocks in chloroform were transferred to a glass test tube and the organic solvent was carefully evaporated using N_2 gas. The resulting lipid films were fully dried on a lyophilizer overnight. Then, multilamellar lipid vesicles were formed by intermittently vortexing the dried films in 50 mM sodium phosphate (pH 7) for 2 h. Resuspended vesicle preparations were treated with three to four cycles of freezing and thawing from a dry ice/ethanol bath to a 42 °C water bath. The preparations were subsequently extruded through a 0.2 μm membrane to form large unilamellar vesicles (LUVs) and incubated overnight at room temperature. The final lipid stock concentration in 50 mM sodium phosphate (pH 7) was 10 or 20 mg/mL. LUV preparations were then incubated with rocking in a 1:1 SDS:lipid ratio for 1.5 h at room temperature. This detergent concentration is sufficient to saturate POPC unilamellar vesicles but not to solubilize them. Then, an appropriate volume of TM3/4 hairpin solubilized in SDS as described above was mixed with the lipid/detergent mixture to a final protein concentration of 5 or 10 μM and a 500:1 lipid:protein ratio. Mixtures were incubated for 1.5 h at room temperature while being rocked. SDS was removed by dialysis and adsorbents, a hybrid method that optimizes detergent removal while minimizing sample loss. Thus, samples were dialyzed four times against ≥200 sample volumes of 50 mM sodium phosphate (pH 7) for ∼24 h for each dialysis. The external buffer of the last three dialyses was supplemented with 1 g of SM-2 Biobeads adsorbent (Bio-Rad) to maximize the removal of the detergent from the dialyzed sample. For Trp quenching experiments in dibrominated POPC analogues (Avanti Polar Lipids), mixtures of 10, 20, 30, and 40% 6,7-BrPC, 9,10-BrPC, or 11,12-BrPC in POPC [1-palmitoyl-2-(6,7-dibromo)stearoyl-*sn*-glycero-3-phosphocholine, 1-palmitoyl-2-(9,10-dibromo)stearoyl-*sn*-glycero-3-phosphocholine, or 1-palmitoyl-2-(11,12-dibromo)stearoyl-*sn*-glycero-3-phosphocholine, respectively] were prepared as described above for pure POPC samples, but lipid stocks of POPC and BrPC in chloroform were mixed and diluted with an additional 1 mL of chloroform to facilitate mixing.

Sodium Dodecyl Sulfate−Polyacrylamide Gel Electrophoresis (SDS−PAGE) and Size-Exclusion Chromatography. Volumes of TM3/4 stocks in SDS containing 2 μg of

protein were mixed with Novex Tris-glycine sample buffer to a concentration of 1× (Life Technologies) and loaded on a Novex 12% NuPAGE Bis-Tris gel (Life Technologies). Gels were run in MES buffer at 200 V and were stained using Coomassie Brilliant Blue. All SDS−PAGE experiments were repeated at least three times.

SEC experiments were performed on a 300 mm × 7.80 mm BioSep-SEC-S3000 column (Phenomenex) in a mobile phase of 0.3% SDS and 50 mM sodium phosphate (pH 7). This column has an exclusion limit of 100 kDa with SDS present in the mobile phase according to the manufacturer's protocol. Twenty-five micrograms of each of the TM3/4 samples was diluted in a final volume of 300 μL with the mobile phase and injected on the column following previous protocols.[17,18] Elution profiles were obtained by measuring the absorbance at 280 nm using a flow rate of 1 mL/min. Gel-phase distribution coefficients (K) were calculated using eq 1:

$$K = (V_e - V_o)/(V_t - V_o) \quad (1)$$

where V_e is the elution volume at the peak of protein absorbance, V_o is the void volume, and V_t is the total bead volume accessible to dissolved solutes. V_o and V_t were estimated from the elution volumes of 0.4 mg of blue dextran (GE Healthcare) and 5% (v/v) β-mercaptoethanol, respectively.

Circular Dichroism Spectroscopy. TM3/4 hairpin constructs solubilized in SDS were diluted to a final protein concentration of 10 μM. For each sample, three accumulated spectra from 250 to 190 nm were recorded on a Jasco J-810 instrument with a 50 nm/min scan speed, a 1 nm bandwidth, a 4 s response time , and a 0.1 cm path length. Spectra of samples reconstituted in lipid bilayers were obtained with 5 μM protein and a 500:1 lipid:protein ratio using a 2 nm bandwidth and 5−15 accumulations. Blank spectra without protein were subtracted.

Trp Fluorescence Spectroscopy. TM3/4 hairpins solubilized in SDS or reconstituted in lipid bilayers were diluted to a final protein concentration of 5 or 10 μM. Trp fluorescence emission spectra were obtained on a Hitachi F-400 Photon Technology International C-60 fluorescence spectrometer in a 1 cm path-length cuvette, using an excitation wavelength of 280 nm, and monitoring emission in a single accumulation from 300 to 380 nm with a step size of 0.5 nm, and an integration time of 1 s. Slits were set to 1 nm for excitation and 3 nm for emission. Blank spectra without protein were subtracted.

Fluorescence quenching data were obtained on a SpectraMax Gemini EM microplate spectrofluorometer (Molecular Devices), reading from the top of 96-well opaque plates. Each well contained 250 μL of 5 μM protein (500:1 lipid:protein ratio). Trp residues were excited at 280 nm, and emission was scanned from 300 to 380 nm as an average of six accumulations with a 1 nm step size and medium photomultiplier tube sensitivity. The area under the full spectrum was used as a measure of intensity after subtracting a blank spectrum from a sample without protein. For the Stern−Volmer analysis,[19] the ratio of fluorescence intensity without quencher and with quencher (F_o/F) was plotted versus quencher concentration. The magnitude of a positive linear relationship between these variables was recognized as the level of quenching by a given quencher. All regression analyses were performed using OriginPro version 8.0. Bovine serum albumin (BSA, Sigma-Aldrich) was used as a negative control for insertion into POPC bilayers.

RESULTS

Pro and Gly Are Common Residues Found in Short Turns of β-Barrel Membrane Proteins. A structural signature of β-barrel folds is the nearly ∼180° change in polypeptide backbone direction that must be effected to allow β-strand formation within the membrane core, a task often accomplished with very short sequences[20] (Figure 1A). To examine the amino acid residues compatible with this change in polypeptide backbone direction, we performed a structural alignment of 623 β-hairpins derived from 48 nonredundant β-barrel structures (Figure 1B; see Experimental Procedures and

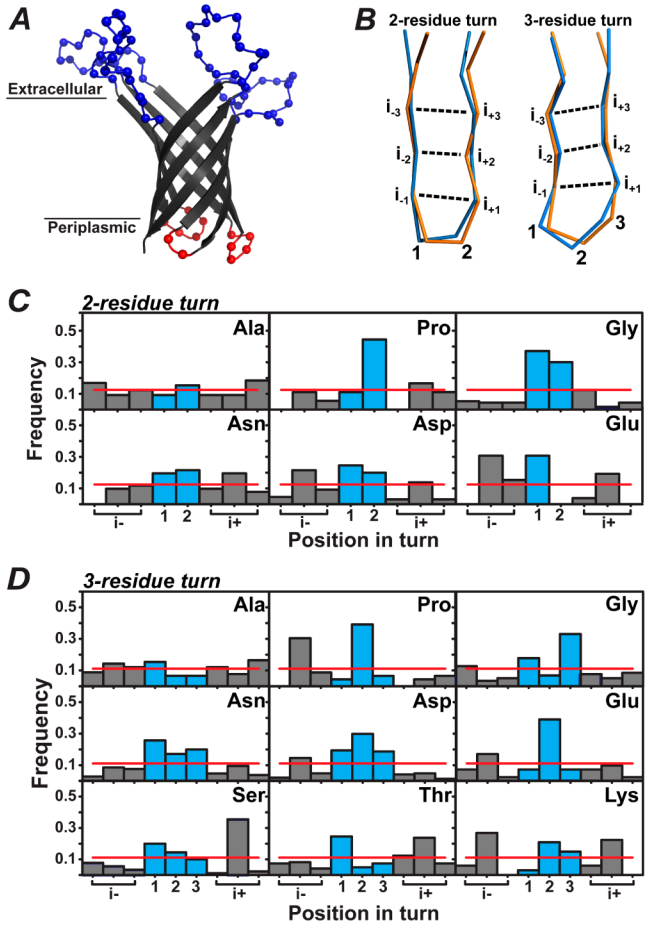

Figure 1. Evaluation of residue frequency in the short loops of β-barrel membrane proteins. (A) Structure of a characteristic β-barrel membrane protein, OmpA (PDB entry 2GE4). Extracellular and periplasmic loops are colored blue and red, respectively, and each loop residue is labeled with a sphere. (B) Structural alignment of β-hairpins from 48 nonredundant β-barrel structures. Hairpins were aligned using the backbone structure of the three H-bonded residues in the β-sheet conformation (anchor residues, labeled i_{-3}/i_{+3}, i_{-2}/i_{+2}, and i_{-1}/i_{+1}) that directly preceded and followed the polypeptide chain region that changed direction by ∼180° (turn residues, numbered). As examples, two-hairpin alignments are shown for 2- and 3-residue turns. (C and D) Residues observed frequently in 2-residue and 3-residue turns, respectively. The frequency of finding a residue at each position of the alignment is indicated relative to a random distribution across all positions (red line; see Experimental Procedures for calculations). Data for β-strand and turn residues are colored gray and blue, respectively. Compared to Ala, a residue with no preference for turn or strand, Pro and Gly are more frequently found in 2- and 3-residue turns than in the adjacent β-strands.

dx.doi.org/10.1021/bi400187w | Biochemistry 2013, 52, 2419−2426

Table 1. Mutagenesis of the TM3/4 Loop with Turn-Inducing Mutations and Its Structural Outcome in SDS

TM3/4 mutant	CFTR TM3/4 loop region*	SDS-PAGE oligomers†	Secondary structure‡	Trp fluorescence peak position (nm)§	
				in SDS	in POPC
WT	^{215}IWELLQASA^{223}	-	α	340	331
PGins216	-IW**PG**ELLQASA-	+++	β	338	331
PGins218	-IWEL**PG**LQASA-	+++	β	338	330
PGins221	-IWELLQA**PG**SA-	-	α	341	330
PGsub218	-IWE**PG**QASA-	+++	β	nd	nd
PGsub221	-IWELLQ**PG**A-	-	α	nd	nd

*The loop predicted for the WT TM3/4 sequence is centered around the residues highlighted in gray.[17] Mutations made in each construct are shown in bold. Residue numbering from the human CFTR sequence is shown for the wild type. PG mutants are designated on the basis of the site of sequence change with reference to the position of proline. †Level of oligomerization of TM3/4 constructs on the SDS−PAGE gel. A dash indicates a monomeric species is present. Three pluses indicate that several oligomeric species are present on the SDS−PAGE gel. ‡Secondary structure of TM3/4 mutants in SDS micelles as determined from circular dichroism spectroscopy. α and β indicate that constructs adopt α-helical and β-sheet structure, respectively. §Positions of Trp fluorescence maxima upon reconstitution of TM3/4 constructs in detergent micelles and lipid bilayers. Average values from three to four replicates are shown. The standard deviation is less than ±1 nm for all samples. Peak positions observed in POPC are statistically different from those observed in SDS ($p < 0.01$). nd, not determined.

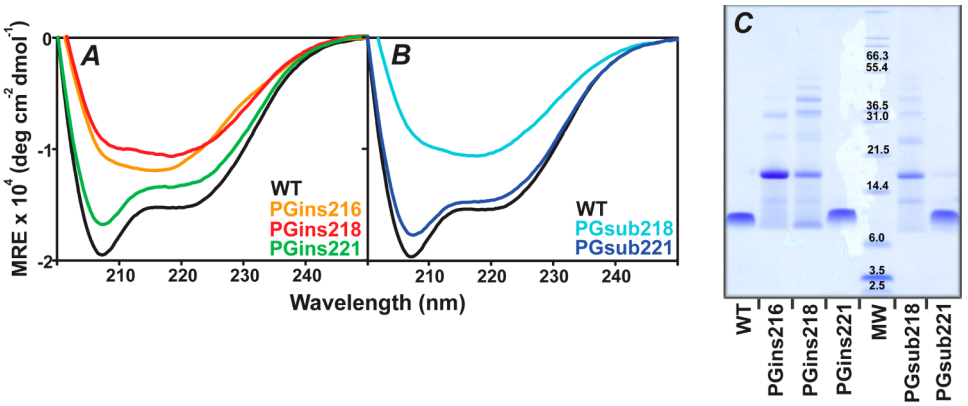

Figure 2. Secondary structure and oligomerization of Pro-Gly TM3/4 loop mutants in a membrane-mimetic environment. Circular dichroism spectra of (A) of PGins mutants and (B) PGsub mutants in 0.3% SDS and 50 mM sodium phosphate (pH 7). An average of three to five replicate measurements is shown. Positioning of Pro-Gly doublets in the TM3/4 loop dictates the conversion from an α-helical to a β-sheet structure in SDS micelles. (C) SDS−PAGE migration of WT TM3/4 and Pro-Gly loop mutants. The positions and molecular masses of protein standards are given. Mutant constructs with a β-sheet CD spectrum form oligomeric ladders.

Figures S1 and S2 of the Supporting Information for details). In β-hairpins where the change in polypeptide chain direction is effected over two residues (Figure 1C), five residues were found to occur more frequently than predicted on the basis of their overall frequency of occurrence in the database (Pro, Gly, Asn, Asp, and Glu), with Pro observed most frequently at position 2 and Gly occurring at a high frequency at both turn positions.

For hairpins in which reversal of polypeptide backbone direction is effected by three residues, greater sequence variation is observed, with eight amino acids occurring at frequencies greater than expected on the basis of their database representation (Figure 1D): Pro, Gly, Asn, Asp, Glu, Ser, Thr, and Lys. Here, Pro (in position 2), Gly (in position 3), and Glu (in position 2) are the most frequently occurring residues. Thus, for both 2- and 3-residue turns, the well-known β-turn formers[16] Pro and Gly are favored, along with some small polar amino acids. Overall, residues with a strong propensity to exist in very defined regions of the Ramachandran plot[21] and strongly favorable to β-turn formation[16] appear to promote polypeptide backbone reversal in short loops of β-barrel proteins.

Design of Short Turn-Inducing Mutations in the TM3/4 Loop. The high frequency of occurrence of Pro and Gly residues in β-barrel loops led us to hypothesize that introduction of these residues into the loop region of a helix−loop−helix TM protein might similarly induce a sharp turn between the two adjacent TM helices. Pro-Gly doublets were accordingly introduced at several positions in the predicted loop region of an 87-residue helix−loop−helix fragment of human CFTR containing TM helices 3 and 4. Because no high-resolution structure of full-length CFTR or of the present hairpin construct is available, we used the consensus output of various TM segment prediction programs[17] to define the TM3 and TM4 start and end sites and considered the intervening region connecting the two TM segments as the TM3/4 loop (sequence centered on ^{217}ELLQA^{221}). We analyzed two sets of mutants. First, Pro-Gly residues were inserted at three different positions, effectively scanning the length of the short TM3/4 loop (Table 1, PGins mutants). These mutations do not change the surrounding residues of the native sequence but instead extend the TM3/4 loop length. Second, we designed substitution mutations (PGsub mutants) that leave loop length unaffected but do alter the sequence hydrophobicity of the loop region, a known factor in membrane

protein folding;[1,17,18,22] for example, PG replaces LL in PGsub218. All Pro-Gly-containing mutants were successfully expressed and purified in milligram amounts (see Experimental Procedures) and typically soluble at concentrations of >2 mg/mL in 0.3% sodium dodecyl sulfate (SDS) and 50 mM sodium phosphate (pH 7).

The Pro-Gly Doublet Induces a Global TM3/4 Structural Change in SDS Micelles. Circular dichroism (CD) spectroscopy was used to evaluate the consequences of introducing the Pro-Gly doublet into the TM3/4 loop region. The WT TM3/4 protein adopts an α-helical structure in SDS as indicated by the double-lobed spectrum with minima around 208 and 222 nm (Figure 2A,B). This secondary structure was relatively unperturbed in the PGins221 and PGsub221 mutants (Figure 2A,B, and Table 1). However, we were intrigued to observe that three Pro-Gly mutations (PGins216, PGins218, and PGsub218) caused a global structural change of TM3/4 from α-helix to predominantly β-sheet structure, with a single minimum in CD spectra centered at 216−218 nm. This result was unanticipated given that each of the >100 variants of TM3/4 that have been characterized to date[17,18,23−25] retained helical structure in SDS, even when various loop substitutions were introduced. Interestingly, this drastic switch in secondary structure observed appears to be dependent on the specific position of the Pro-Gly mutations within the loop.

TM3/4 β-Sheet Oligomers Are Not Random Aggregates. A change in CD readouts of secondary structure from α to β is often accompanied by a loss of solubility and/or nonspecific protein aggregation. We therefore investigated whether the observed switch in the secondary structure of the PGins216, PGins218, and PGsub218 mutants arose from a change in their solubility properties. First, the oligomeric states of WT and all Pro-Gly mutants in SDS were evaluated via SDS−PAGE. We observed that the TM3/4 constructs remaining α-helical in CD spectra appear monomeric on the SDS−PAGE gel (Figure 2C). However, the PGins216, PGins218, and PGsub218 mutants each formed ladders of discrete oligomers on the SDS−PAGE gel (Figure 2C), while evidence of macroscopic aggregation (i.e., precipitate, cloudiness) was absent, even in concentrated samples (up to ∼10 mg/mL). Importantly, the formation of oligomers on gels accompanies CD-determined α-helical-to-β-sheet secondary structure conversion in the SDS environment.

Evidence of large aggregates was similarly absent in the size-exclusion chromatography (SEC) elution profiles of the WT and β-sheet oligomeric mutants (PGins216, PGins218, and PGsub218) solubilized in SDS (Figure S3 of the Supporting Information), where aggregates larger than the exclusion limit of the SEC column [V_o ∼ 100 kDa in SDS (see Experimental Procedures)] were not observed. Further, during storage in SDS for 1 month at room temperature, conditions that can promote nonspecific membrane protein aggregation, we found that the CD spectra of WT and each Pro-Gly mutant (Figure S4A−C of the Supporting Information) were largely comparable to the original determinations and retain their secondary structure patterns. It is noted, however, that over this 1 month period, PGsub221 loses a discernible fraction of its helicity (compare Figure 2B with Figure S4B of the Supporting Information). In addition, minimal changes in the relative content of oligomeric species do appear over time on SDS−PAGE gels: while WT remains monomeric, PGins221 and PGsub221 slowly gain small populations of larger species (compare Figure 2C with Figure S4D of the Supporting Information).

Folding of TM3/4 Mutants in Lipid Bilayers. Having characterized the secondary structures of the TM3/4 loop mutants in SDS, we inquired whether a switch from helix to sheet secondary structure would occur for this set of mutants in the nativelike context of a lipid bilayer, an environment more restrictive for protein structure than SDS micelles. Accordingly, the CD spectra of WT and Pro-Gly insertion mutants were obtained after reconstitution into 1-palmitoyl-2-oleoyl-*sn*-glycero-3-phosphocholine (POPC) vesicles (see Experimental Procedures). The CD spectrum of the WT and PGins221 sequence remained consistent with a largely α-helical conformation under these conditions. The spectral change observed for the WT toward a more "classical" α-helical pattern in POPC (Figure 3A) is consistent with the membrane-spanning orientation deduced for WT TM3/4 from the brominated lipid experiments (vide infra). The spectra of the Pro-Gly doublet mutants PGins216 and PGins218 remained consistent with β-sheet structure.

Membrane Insertion of TM3/4 Constructs Studied by Trp Fluorescence. To determine the depth of penetration of the WT and mutant TM3/4 proteins into bilayers, we used Trp fluorescence spectroscopy, utilizing blue shifts that arise as a function of the polarity of the Trp environment, and its sensitivity to proximal quenching agents.[19] All TM3/4 constructs have two native Trp residues that could be utilized as probes of bilayer position (Figure 3B). We initially examined the blue shift in the Trp fluorescence emission peak by comparing the maximal wavelengths of the SDS and POPC bilayer-solubilized proteins. We found that peak positions of TM3/4 constructs in SDS varied from 338 to 341 nm (Table 1), with all values strongly blue-shifted from the wavelength for free Trp in water (∼355 nm[19]) (gray line in Figure 3C). Further, blue shifts significantly increase for the corresponding constructs upon reconstitution in POPC bilayers relative to the SDS-solubilized state (Figure 3C), providing evidence of the embedding of (at least one) TM3/4 Trp residue in the hydrophobic microenvironment of the lipid vesicles.

However, Trp blue shift data were unable to distinguish whether the α-helical or the β-sheet TM3/4 constructs were incorporated into POPC vesicles in a manner parallel or perpendicular to the bilayer normal. To address this situation, we used position-specific collisional quenchers of fluorescence to evaluate the position of Trp residues relative to the bilayer lipids. Three dibrominated POPC analogues [6,7-, 9,10-, and 11,12-BrPCs (see Experimental Procedures)] with Br substituents 11.0, 8.3, and 6.5 Å from the bilayer midpoint, respectively,[26,27] were used at increasing mole percents in vesicle preparations to assess quenching at various positions within the hydrophobic core of the membrane. Stern−Volmer analysis[19] for WT TM3/4 in the presence of increasing concentrations of quencher (Figure S5 of the Supporting Information) established that at least one Trp residue of WT TM3/4 could be quenched by each of the three brominated positions of the BrPC lipids (Figure 3D), a result consistent with its incorporation at positions proximal to both POPC headgroup regions and tail group regions near the bilayer midpoint. This result strongly suggests a transmembrane orientation for WT TM3/4. However, the Trp residues of the β-sheet-type PGins216 TM3/4 were quenched by 6,7-BrPC (∼25% vs WT TM3/4), but not by the 9,10- and 11,12-BrPC lipids (Figure 3D). This finding implies that the PGins216

dx.doi.org/10.1021/bi400187w | *Biochemistry* 2013, 52, 2419−2426

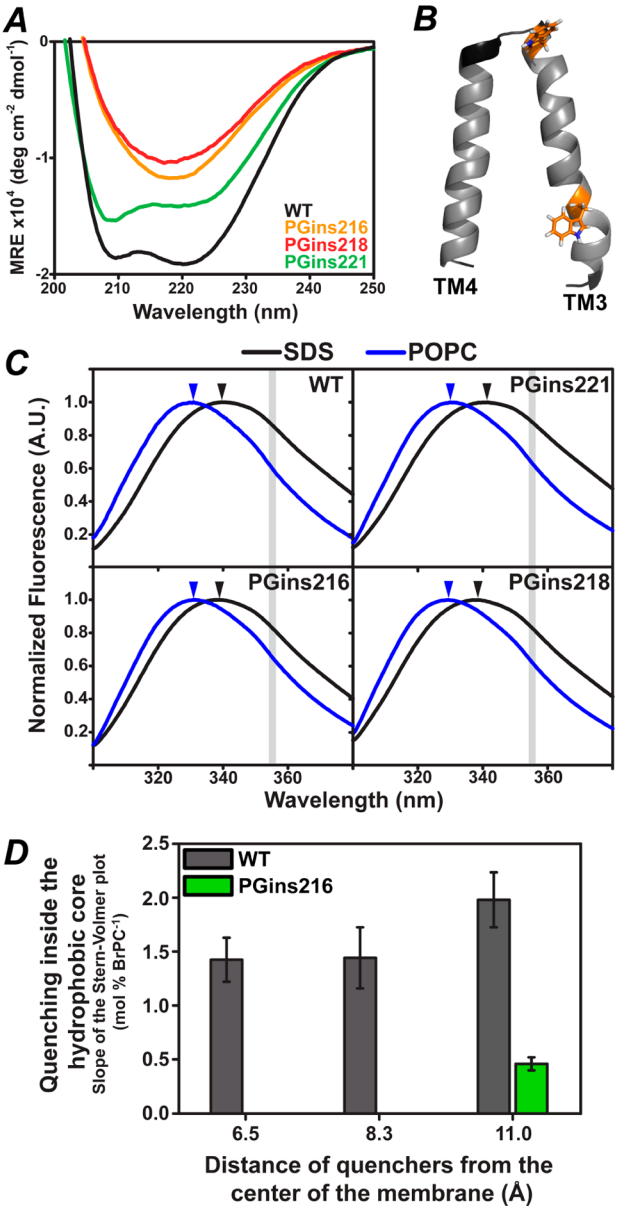

Figure 3. Circular dichroism and fluorescence spectroscopy of TM3/4 Pro-Gly mutants in lipid bilayers. (A) CD spectra of WT and PG insertion mutants after reconstitution of TM3/4 hairpins in POPC vesicles. An average of three or four replicate measurements is shown. WT TM3/4 and PGins221 hairpins adopt an α-helical structure in the presence of POPC vesicles, while other constructs display spectra consistent with β-structure. (B) Localization of the two native Trp residues (orange sticks) in the TM3/4 sequence excerpted from a homology model of full-length CFTR.[39] Residues predicted to be membrane-embedded are colored gray.[17] (C) Trp fluorescence spectra of Pro-Gly insertion mutants and WT TM3/4 in the presence of SDS micelles and POPC bilayers. An average of three or four replicate measurements is shown. A stronger blue shift was observed in all constructs in POPC vesicles relative to samples in SDS micelles (Table 1). The canonical peak position of Trp in water (~355 nm) is indicated by a gray line.[19] (D) Quenching of Trp fluorescence by brominated phosphatidylcholine probes (see Experimental Procedures). Slopes of Stern–Volmer plots are given on the y-axis for WT and PGins216 TM3/4 (also see Figure S5 of the Supporting Information). Larger slope values indicate increased effects of quenchers on Trp fluorescence. The propagated error is shown as error bars on each data point. An average of three replicate measurements was used for the analysis.

mutant does not penetrate deeply into the midpoint of the bilayer core but remains associated with headgroup-proximal hydrophobic regions. The observed level of quenching of the PGins216 mutant is nonetheless an indication of a substantive level of bilayer association, as no Trp quenching by BrPCs was observed in a negative control of insertion [BSA (Figure S5 of the Supporting Information)].

DISCUSSION

Pro-Gly Loop Mutations Induce Secondary Structure Conversion in TM3/4 Hairpins. Extensive mutational analysis in α-helical transmembrane segments has shown that sequence changes within TM helices can affect quaternary structure,[1,4] lipid bilayer insertion,[2] and/or stability,[1] but mutations that completely convert secondary structure are rare. Even Pro and Gly, known α-helix breakers in water-soluble proteins, can be well-accommodated by TM helices solubilized in a hydrophobic environment.[28−30] In this work, we observed that incorporation of a Pro-Gly doublet, residues associated with sharp turns in loops of natural β-barrel membrane proteins, at selected positions within the loop of a helix−loop−helix membrane protein causes a change in the secondary structure of its transmembrane regions from α-helical to β-sheet. This transformation occurs both in the presence of SDS micelles and in POPC bilayers. Such a drastic structural change has been observed for small water-soluble proteins in few instances because of mutations[31,32] and in small cell-penetrating peptides upon membrane insertion.[33,34] However, a complete change in the fold with such a minimal number of mutations[35] has not previously been observed for a membrane protein to the best of our knowledge.

Effect of a Short Turn on an α-Helical Hairpin Conformation. The WT TM3/4 loop sequence has ostensibly been optimized to allow for the formation and likely interaction of two adjacent α-helical TM segments 3 and 4 (Figure 4A), yet suitably positioned Pro-Gly residues in the TM3/4 loop may be too constraining on TM3 and TM4 for proper α-helical hairpin packing (Figure 4D), perhaps producing severe steric clashes between the two adjacent helices. With the imposition of such a structurally restricting loop, we observed that several mutated TM3/4 constructs switch to a stable β-hairpin structure (Figure 4B). Given that a nascent "monomeric" β-hairpin structure can be unstable in detergent micelles or in a lipid bilayer because of free polar backbone amides and carbonyls in a hydrophobic environment, oligomerization of Pro-Gly TM3/4 as observed in SDS−PAGE experiments would minimize unsatisfied backbone H-bonds and act to preserve solubility (Figure 4C). Various oligomeric conformations are conceivable here, with a combination of β-hairpins forming sheets laterally and/or also stacking through side chain−side chain interactions. In principle, our observation of insertion of a partial protein into the more restrictive environment of POPC bilayers could indicate the formation of similar oligomeric structures (Figure 4E) or perhaps the internalization of Trp residue(s) in at least some population of primitive β-barrel structures analogous to oligomeric β-hairpin structures known in nature.[36,37] Because the observed β-sheet structures are always initiated through solubilization in detergents, it remains possible that the secondary structure(s) observed could reflect the existence, at least in part, of kinetically trapped intermediates in micelles during TM3/4 folding.

Sequence Dependence of Pro-Gly-Induced β-Sheet Structures. From our analysis of short turns of β-barrel

dx.doi.org/10.1021/bi400187w | Biochemistry 2013, 52, 2419−2426

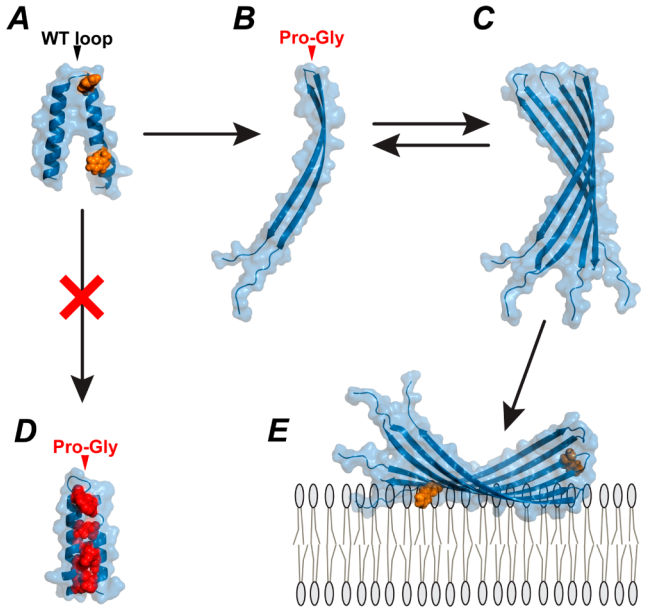

Figure 4. Model for the secondary structure conversion of TM3/4 hairpins promoted by turn-inducing loop mutations. Protein and lipid structures are drawn to scale. The two Trp residues present in the native TM3/4 sequence are colored orange. (A) WT TM3/4 hairpin structural model extracted from a full-length CFTR homology model.[39] (B) A structurally constrained loop sequence in a TM3/4 α-helical hairpin may favor a conformational switch to a β-hairpin structure. (C) Oligomerization of TM3/4 β-hairpins would be strongly favored in a hydrophobic environment because of the presence of unsatisfied backbone H-bonds. (D) Accommodating a short turn in the TM3/4 loop due to proper positioning of Pro-Gly residues may cause a steric clash (colored red) between TM3 and TM4 helices and not allow proper helix–helix packing. (E) TM3/4 β-Sheet oligomers can interact with lipid bilayers during reconstitution in a membrane interface-embedded conformation, but the nonoptimal TM3/4 sequence is likely not compatible with full transmembrane insertion.

membrane proteins (vide infra), no clear local sequence pattern around loop residues suggests a formal positional dependence of Pro-Gly-induced formation of β-sheet structures. However, we observed that secondary structure conversion occurs in TM3/4 constructs only when β-turn-promoting Pro-Gly residues are positioned either at the C-terminal region of the TM3 segment or in the middle of the TM3/4 loop; the doublet has minimal structural switching power when it initiates the TM4 segment. Such a stark positional preference within a relatively short loop is likely a consequence of local TM3/4 sequence features. Understandably, the native helical TM sequences in WT TM3/4 would not be optimal for facile packing into a β-hairpin. In addition, helical TM structures and β-sheet segments are not comparable in overall length when spanning membranes (viz., ~20 residues are required to span the bilayer in a TM helix vs the ~12-residue span that is required for a β-strand[20]), nor do the native TM3/4 helices feature an obvious alternating nonpolar–polar sequence motif,[20] a pattern observed in some β-barrel structures that acts to accommodate a lipid-facing surface inside the membrane. Thus, the nucleating effect of Pro-Gly positioning in the TM3/4 loop could result from its modulation of TM segment hydrophobic patterning, where only certain sets of TM3 and TM4 residues are placed in suitable register to support β-type packing. An additional factor that may influence Pro-Gly structural effects is the potential consequence of the propensity of N-terminal Pro residues (i.e., with respect to the TM4 helix) to initiate helical conformation.[38]

In conclusion, given the innate sensitivity we observed of helical folds to the sequence of short loop regions, such loops in membrane proteins appear to function as connectors that allow for adequate reversal of the polypeptide chain and proper folding of the adjacent membrane-embedded regions. As such, the facile α-helix to β-sheet conversions reported here identify a specific contribution of membrane protein loops to overall protein stability.

■ ASSOCIATED CONTENT

Supporting Information

Complete results of the frequency analysis of residues in short turns of β-barrels, size-exclusion chromatography profiles of oligomeric β-sheet TM3/4 mutants, time stability analysis of Pro-Gly TM3/4 mutants in detergents, Trp fluorescence peak shift analysis of PGins constructs in SDS, and Stern–Volmer analysis of position-specific Trp fluorescence quenching. This material is available free of charge via the Internet at http://pubs.acs.org.

■ AUTHOR INFORMATION

Corresponding Author

*Research Institute, Hospital for Sick Children, 555 University Ave., Toronto, Ontario M5G 1X8, Canada. Phone: (416) 813-5924. E-mail: deber@sickkids.ca.

Funding

This work was supported, in part, by a grant to C.M.D. from Cystic Fibrosis Canada. V.G.N. is the recipient of a Doctoral Training Award from the Fonds de la Recherche en Santé du Québec (FRSQ) and a Banting and Best Canada Graduate Scholarship from the Canadian Institutes of Health Research (CIHR).

Notes

The authors declare no competing financial interest.

■ ACKNOWLEDGMENTS

We thank Arianna Rath for constructing the alignment of β-hairpin structures and for critical editing of the manuscript and Derek Ng and David Tulumello for useful discussions. We also thank Yohei Norimatsu (Oregon Health & Science University, Portland, OR) for providing us with his CFTR homology model.

■ ABBREVIATIONS

TM, transmembrane; CFTR, cystic fibrosis transmembrane conductance regulator; TM3/4, transmembrane segments 3 and 4; SDS, sodium dodecyl sulfate; POPC, 1-palmitoyl-2-oleoyl-*sn*-glycero-3-phosphocholine; 6,7-BrPC, 1-palmitoyl-2-(6,7-dibromo)stearoyl-*sn*-glycero-3-phosphocholine; 9,10-BrPC, 1-palmitoyl-2-(9,10-dibromo)stearoyl-*sn*-glycero-3-phosphocholine; 11,12-BrPC, 1-palmitoyl-2-(11,12-dibromo)-stearoyl-*sn*-glycero-3-phosphocholine; HFIP, 1,1,1,3,3,3-hexafluoro-2-propanol; CD, circular dichroism; SEC, size-exclusion chromatography; V_o, void volume; BSA, bovine serum albumin; RP-HPLC, reverse-phase high-performance liquid chromatography.

■ REFERENCES

(1) Rath, A., and Deber, C. (2012) Protein Structure in Membrane Domains. *Annu. Rev. Biophys. 41*, 135–155.

(2) Hessa, T., Meindl-Beinker, N. M., Bernsel, A., Kim, H., Sato, Y., Lerch-Bader, M., Nilsson, I., White, S. H., and Von Heijne, G. (2007) Molecular code for transmembrane-helix recognition by the Sec61 translocon. *Nature 450*, 1026−1030.
(3) Moon, C. P., and Fleming, K. G. (2011) Side-chain hydrophobicity scale derived from transmembrane protein folding into lipid bilayers. *Proc. Natl. Acad. Sci. U.S.A. 108*, 10174−10177.
(4) Ng, D. P., Poulsen, B. E., and Deber, C. M. (2011) Membrane protein misassembly in disease. *Biochim. Biophys. Acta 1818*, 1118−1122.
(5) Martin, N. P., Leavitt, L. M., Sommers, C. M., and Dumont, M. E. (1999) Assembly of G protein-coupled receptors from fragments: Identification of functional receptors with discontinuities in each of the loops connecting transmembrane segments. *Biochemistry 38*, 682−695.
(6) Marti, T. (1998) Refolding of bacteriorhodopsin from expressed polypeptide fragments. *J. Biol. Chem. 273*, 9312−9322.
(7) Allen, S. J., Kim, J. M., Khorana, H. G., Lu, H., and Booth, P. J. (2001) Structure and function in bacteriorhodopsin: The effect of the interhelical loops on the protein folding kinetics. *J. Mol. Biol. 308*, 423−435.
(8) Kim, J. M., Booth, P. J., Allen, S. J., and Khorana, H. G. (2001) Structure and function in bacteriorhodopsin: The role of the interhelical loops in the folding and stability of bacteriorhodopsin. *J. Mol. Biol. 308*, 409−422.
(9) Ridge, K. D., and Abdulaev, N. G. (2000) Folding and assembly of rhodopsin from expressed fragments. *Methods Enzymol. 315*, 59−70.
(10) Ahuja, S., Hornak, V., Yan, E. C. Y., Syrett, N., Goncalves, J. A., Hirshfeld, A., Ziliox, M., Sakmar, T. P., Sheves, M., Reeves, P. J., Smith, S. O., and Eilers, M. (2009) Helix movement is coupled to displacement of the second extracellular loop in rhodopsin activation. *Nat. Struct. Mol. Biol. 16*, 168−175.
(11) Dmitriev, O. Y., and Fillingame, R. H. (2007) The rigid connecting loop stabilizes hairpin folding of the two helices of the ATP synthase subunitc. *Protein Sci. 16*, 2118−2122.
(12) Yeagle, P. L., Alderfer, J. L., Salloum, A. C., Ali, L., and Albert, A. D. (1997) The first and second cytoplasmic loops of the G-protein receptor, rhodopsin, independently form β-turns. *Biochemistry 36*, 3864−3869.
(13) Bennett, M., Yeagle, J. A., Maciejewski, M., Ocampo, J., and Yeagle, P. L. (2004) Stability of loops in the structure of lactose permease. *Biochemistry 43*, 12829−12837.
(14) Katragadda, M., Alderfer, J. L., and Yeagle, P. L. (2000) Solution structure of the loops of bacteriorhodopsin closely resembles the crystal structure. *Biochim. Biophys. Acta 1466*, 1−6.
(15) Marcelino, A. M. C., and Gierasch, L. M. (2008) Roles of β-turns in protein folding: From peptide models to protein engineering. *Biopolymers 89*, 380−391.
(16) Hutchinson, E. G., and Thornton, J. M. (1994) A revised set of potentials for β-turn formation in proteins. *Protein Sci. 3*, 2207−2216.
(17) Nadeau, V. G., Rath, A., and Deber, C. M. (2012) Sequence Hydropathy Dominates Membrane Protein Response to Detergent Solubilization. *Biochemistry 51*, 6228−6237.
(18) Rath, A., Glibowicka, M., Nadeau, V. G., Chen, G., and Deber, C. M. (2009) Detergent binding explains anomalous SDS-PAGE migration of membrane proteins. *Proc. Natl. Acad. Sci. U.S.A. 106*, 1760−1765.
(19) Lakowicz, J. R. (2006) Quenching of fluorescence. In *Principles of fluorescence spectroscopy*, 3rd ed., pp 277−327, Springer, New York.
(20) Wimley, W. C. (2003) The versatile β-barrel membrane protein. *Curr. Opin. Struct. Biol. 13*, 404−411.
(21) Shortle, D. (2002) Composites of local structure propensities: Evidence for local encoding of long-range structure. *Protein Sci. 11*, 18−26.
(22) Tulumello, D. V., and Deber, C. M. (2011) Positions of polar amino acids alter interactions between transmembrane segments and detergents. *Biochemistry 50*, 3928−3935.
(23) Choi, M. Y., Cardarelli, L., Therien, A. G., and Deber, C. M. (2004) Non-native interhelical hydrogen bonds in the cystic fibrosis transmembrane conductance regulator domain modulated by polar mutations. *Biochemistry 43*, 8077−8083.
(24) Mulvihill, C. M., and Deber, C. M. (2010) Evidence that the translocon may function as a hydropathy partitioning filter. *Biochim. Biophys. Acta 1798*, 1995−1998.
(25) Wehbi, H., Rath, A., Glibowicka, M., and Deber, C. M. (2007) Role of the extracellular loop in the folding of a CFTR transmembrane helical hairpin. *Biochemistry 46*, 7099−7106.
(26) McIntosh, T. J., and Holloway, P. W. (1987) Determination of the depth of bromine atoms in bilayers formed from bromolipid probes. *Biochemistry 26*, 1783−1788.
(27) Kleinschmidt, J. H., and Tamm, L. K. (1999) Time-resolved distance determination by tryptophan fluorescence quenching: Probing intermediates in membrane protein folding. *Biochemistry 38*, 4996−5005.
(28) Liu, L. P., Li, S. C., Goto, N. K., and Deber, C. M. (1996) Threshold hydrophobicity dictates helical conformations of peptides in membrane environments. *Biopolymers 39*, 465−470.
(29) Li, S. C., Goto, N. K., Williams, K. A., and Deber, C. M. (1996) α-Helical, but not β-sheet, propensity of proline is determined by peptide environment. *Proc. Natl. Acad. Sci. U.S.A. 93*, 6676−6681.
(30) Yohannan, S., Faham, S., Yang, D., Whitelegge, J. P., and Bowie, J. U. (2004) The evolution of transmembrane helix kinks and the structural diversity of G protein-coupled receptors. *Proc. Natl. Acad. Sci. U.S.A. 101*, 959−963.
(31) Dalal, S., Balasubramanian, S., and Regan, L. (1997) Protein alchemy: Changing β-sheet into α-helix. *Nat. Struct. Biol. 4*, 548−552.
(32) Alexander, P. A., He, Y., Chen, Y., Orban, J., and Bryan, P. N. (2009) A minimal sequence code for switching protein structure and function. *Proc. Natl. Acad. Sci. U.S.A. 106*, 21149−21154.
(33) Magzoub, M., Kilk, K., Eriksson, L. E., Langel, U., and Gräslund, A. (2001) Interaction and structure induction of cell-penetrating peptides in the presence of phospholipid vesicles. *Biochim. Biophys. Acta 1512*, 77−89.
(34) Reshetnyak, Y. K., Segala, M., Andreev, O. A., and Engelman, D. M. (2007) A Monomeric Membrane Peptide that Lives in Three Worlds: In Solution, Attached to, and Inserted across Lipid Bilayers. *Biophys. J. 93*, 2363−2372.
(35) Rose, G. (1997) Protein folding and the Paracelsus challenge. *Nat. Struct. Biol. 4*, 512−514.
(36) Song, L., Hobaugh, M. R., Shustak, C., Cheley, S., Bayley, H., and Gouaux, J. E. (1996) Structure of staphylococcal α-hemolysin, a heptameric transmembrane pore. *Science 274*, 1859−1866.
(37) De, S., and Olson, R. (2011) Crystal structure of the *Vibrio cholerae* cytolysin heptamer reveals common features among disparate pore-forming toxins. *Proc. Natl. Acad. Sci. U.S.A. 108*, 7385−7390.
(38) Aurora, R., and Rose, G. D. (1998) Helix capping. *Protein Sci. 7*, 21−38.
(39) Norimatsu, Y., Ivetac, A., Alexander, C., Kirkham, J., Donnell, N. O., Dawson, D. C., and Sansom, M. S. P. (2012) Cystic Fibrosis Transmembrane Conductance Regulator: A Molecular Model Defines the Architecture of the Anion Conduction Path and Locates a "Bottleneck" in the Pore. *Biochemistry 51*, 2199−2212.